Simultaneous determination of intramolecular distance distributions and conformational dynamics by global analysis of energy transfer measurements

Joseph M. Beechem* and Elisha Haas‡

*The University of Illinois Urbana-Champaign, Department of Physics, Laboratory for Fluorescence Dynamics, Urbana, Illinois 61801; and ‡Department of Life Sciences, Bar-Ilan University, Ramat-Gan 52100, and ‡Department of Chemical Physics and Biophysics, The Weizmann Institute of Science, Rehovot 76100, Israel

ABSTRACT Fluorescence energy transfer is widely used for determination of intramolecular distances in macromolecules. The time dependence of the rate of energy transfer is a function of the donor/acceptor distance distribution and fluctuations between the various conformations which may occur during the lifetime of the excited state. Previous attempts to recover both distance distributions and segmental diffusion from time-resolved experiments have been unsuccessful due to the extreme correlation between fitting parameters. A method has been developed, based on global analysis of both donor and acceptor fluorescence decay curves, which overcomes this extreme cross-correlation and allows the parameters of the equilibrium distance distributions and intramolecular diffusion constants to be recovered with high statistical significance and accuracy. Simulation studies of typical intramolecular energy transfer experiments reveal that both static and dynamic conformational distribution information can thus be obtained at a single temperature and viscosity.

INTRODUCTION

The determination of the equilibrium distribution of conformational states of macromolecules and the time dependence of interconversion is of central interest in understanding how structure and dynamics contribute to biological activity (1–4). Fast interconversions of equilibrium conformers may provide the basis for the local and global conformational transitions important for many biochemical reactions. Such fast motions have been the focus of many theoretical studies and molecular dynamics simulations. Conformational distributions and dynamic motions can be examined by studying "local" dynamics, involving a small number of bond angles and rates of rotations, or by studying the segmental or global motions of entire domains of macromolecules. A relatively limited number of experimental results which characterize global conformational changes in terms of structural fluctuations are available. This is primarily due to the technical difficulties involved in measurement of rates and extents of continuous random conformational fluctuations occurring within a population of macromolecules at equilibrium (5). Examination of conformational distributions using nonradiative energy transfer measurements is attractive because the effect of both distance (and angular) fluctuations on the rate of transfer can be accurately calculated (6, 7).

It has been shown that the time dependence of the rates of nonradiative energy transfer between probes attached to well defined sites on peptides and proteins is a function of both the distribution of distances between the labeled sites and the rates of conformational interconversions (8–10). The probability, $n_{D\to A}$, of energy transfer from donor D to acceptor A is given by (6)

$$n_{D\to A} = \frac{9000(\ln 10)\kappa^2\eta_o}{128\pi^5 n^4 N r^6 \tau}\int_0^\infty \frac{f(\bar{\nu})\epsilon(\bar{\nu})}{\bar{\nu}^4}\,d\bar{\nu} = 1/\tau(R_o/r)^6, \quad (1)$$

where η_o is the quantum yield of the donor in the absence of an acceptor, n is the refractive index of the medium, N is Avogadro's number, τ is the excited-state lifetime of the donor, r is the distance between the donor and acceptor, $F(\bar{\nu})d\bar{\nu}$ is the normalized fluorescence intensity of the donor in the wavenumber range $\bar{\nu}$ to $\bar{\nu} + d\bar{\nu}$, $\epsilon(\bar{\nu})$ is the absorption coefficient of the acceptor at the wavenumber $\bar{\nu}$, R_o (as defined by Eq. 1) is the distance between D and A when transfer efficiency is 50%, and κ^2 is a factor that expresses the orientational dependence of the probability of energy transfer.

The efficiency of energy transfer measured by steady-state methods represents an average quantity from which $N_o(r)$, the equilibrium interprobe distance distribution, cannot be obtained. Examination of the kinetics of the fluorescence decay of the donor or the acceptor, $F_D(t)$ or $F_A(t)$, however, does inherently contain enough information for the determination of $N_o(r)$. The impulse response of the donor's fluorescence (in the absence of diffusion) can be written as

$$F_D(t) = \int_0^\infty \sum_{i=1}^{n} N_o(r)\exp\left[\left(\frac{-t}{\tau_i}(1 + (R_o/r)^6\right)\right]dr, \quad (2)$$

Dr. Beechem's current address is: Vanderbilt University, Dept. of Molecular Physiology and Biophysics, 602 Light Hall, Nashville, TN 37232.

0006-3495/89/06/1225/12 $2.00

where there are n donor lifetimes in the absence of acceptor. Analysis methodologies using this equation have been presented for analyzing the donor fluorescence decay in terms of the equilibrium distance distribution $N_o(r)$ (8, 9, 11–13). Eq. 2, however, does not apply to cases in which the interprobe distances change during the lifetime of the excited state (i.e., typical solution studies of proteins and polypeptides at room temperature). The model equations utilized in this study will directly fit the parameters of a partial differential equation which models the distance distribution(s) and diffusion process simultaneously (Eq. 3).

In a time-resolved fluorescence experiment, one initially observes the decay of energy transfer with distance-dependent rates characterized completely by the ground-state equilibrium distribution ($N_o[r]$). However, due to the steep distance dependence of the energy transfer rate, the population of molecules with a small r decay very quickly. Although the equilibrium distance distribution is not changing, the distribution of distances (as observed by the fluorescence experiment) evolves, so that at longer times, one is selectively observing the population of molecules with large donor/acceptor separations. If the observed molecules experience Brownian motion, one can observe in the decay of the donor fluorescence an enhancement of the donor decay (not predicted by Eq. 2) which reflects the "diffusion" of the large separation donor/acceptor molecules to shorter distances. It is this enhancement of the donor decay, which contains the very important information concerning the Brownian motion of the labeled segments relative to one another. If the effects of Brownian motion are neglected, and Eq. 2 is directly used in the analysis of energy transfer studies on flexible molecules, the recovered $N_o(r)$ will be artificially "biased" to shorter distances to compensate for the increased efficiency of transfer brought about by diffusion of the donor/acceptor pair.

The range of conformational transition rates which can be detected by time-resolved fluorescence spectroscopy depends on the lifetime of the excited state of the donor and can range from as little as 5 ps to as much as 500 ns or more. It has been shown that fluorescence techniques can be extended to measurements of even slower processes by autocorrelation analysis of the fluctuations of the intensity of light emitted by a small sample of labeled molecules observed under constant excitation intensity (10). The emphasis of this paper will be to provide a methodology whereby one can simultaneously determine both the equilibrium distribution of distances and the diffusion coefficient(s) in synthetic and biological macromolecules from time-resolved fluorescence decay curves of donor/acceptor pairs.

A major difficulty in the analysis of the fluorescence experiments (especially those complicated by distributions of fitting parameters) is the ill-defined nature of resolving complex multi- (and distributed) exponential decay functions (14, 15). This severely limits the number of parameters that can be determined from a single decay curve measurement. It has been found that there exists a strong correlation between the parameters that characterize the equilibrium distance distribution(s) and the parameters describing the intramolecular Brownian motion. For this reason, the simultaneous determination of both the equilibrium interprobe distances distribution functions and the rate of conformational transitions has not been possible by examining only the decay kinetics of the donor.

Nonlinear analysis of multiple experiments in terms of internally consistent models has been utilized by many other disciplines (see references 4, 16, 17 for typical examples) but only recently has been widely accepted as beneficial for the analysis of fluorescence decay kinetics. The simultaneous analysis of multiple fluorescence decay experiments is known as "global analysis" and has been shown to increase the accuracy in the recovery of complex decay kinetics (18–24). The original global analysis programs were limited to fitting sums of linked exponential decays (18, 19), but have recently been extended to fit both discrete and distributed physical models (integrated or differential form) (15, 20, 23). The emphasis of these later global analysis programs has been to perform *physical model* fitting rather than empirical fitting of discrete or distributed exponential components. Analysis of energy transfer between donor-acceptor pairs in proteins and polypeptides is an area where distributed fitting parameters are clearly justified. The solution behavior of these molecules involves fluctuations in distances between donor-acceptor pairs and therefore creates a complex pattern of fluorescence decay in both the donor and acceptor regions.

Historically, the decay kinetics of intramolecular energy transfer systems were examined using a long multistep process. Experiments are first performed examining the lifetime of the donor in the absence of the acceptor, to estimate the value of the donor lifetime(s) and amplitude(s). This result becomes a known quantity in the subsequent examination of the decay kinetics of the donor in the presence of the acceptor. Experiments are then performed in the high viscosity limit (low temperatures), where one can uncouple the dynamic diffusion effects from the energy transfer process (25–27). Analysis of these experiments then allowed for the recovery of the distance distribution(s) in the absence of diffusion. This distance distribution, is used as a known quantity in the analysis of the low viscosity solution behavior of the system in terms of energy transfer and diffusion.

The problems and difficulties involved in this type of multistep analysis involve both error propagation terms

and temperature/viscosity extrapolation assumptions (26) on the invariance of the distance distributions. This sequential approach has also been shown to be inadequate for the resolution of closely spaced or complex exponential decay patterns (24). Although there is additional information content concerning diffusion and distance distributions in the decay kinetics of the acceptor, these analyses were not implemented due to the extremely complex nature of the acceptor decay.

In the present study we developed a new method which eliminates the multistep process and overcomes the extreme correlation between the distance distribution and diffusion parameters. It is shown that by global analysis of four experiments, in which the fluorescence decay of the donor and acceptor are measured both in the presence of energy transfer (doubly labeled molecules) and in its absence (singly labeled molecules), all of the physical parameters which characterize the energy transfer system can be obtained. In addition, the parameters are determined from the analysis of decay curves measured at a single temperature/viscosity.

THEORY

The present analysis of fluorescence decay curves for determination of intramolecular distances distributions and rates of intramolecular segmental diffusion are based on theory published elsewhere (9, 25). Consider a population of conformationally distributed molecules, where each molecule is labeled by a single donor and a single acceptor at well-defined unique sites. At equilibrium, the distance between the probes (r), is represented by the radial probability distribution function $N_0(r)$. If the distance distribution is a delta function, then the donor and acceptor decay kinetics observed are simple: single exponential donor decay and double exponential acceptor decay. However, in almost all biophysical systems of interest, the decay kinetics are more complex and must be analyzed using more sophisticated fitting functions. The decay kinetics of donor-acceptor pairs are primarily complicated by two processes: conformational distributions of distances between donor/acceptor pairs and interconversions between the conformational distributions occurring during the lifetime of the excited state.

Consider as a special case, experiments performed where the rate of conformational interconversions are inhibited or nonexistent. At time $t = 0$, a sample of the donor probes is excited by an infinitely short pulse of light. The interprobe distance distribution of the ensemble of molecules with an excited donor probe, $N^*(r, t)$, is initially identical to the population equilibrium interprobe distances distribution, $N_0(r)$, simply due to the random sampling by the excitation transition. Within a very short time after excitation, however, a rapid decay of the donor excited states occurs for the fraction of molecules with short interprobe distances due to the $1/r^6$ enhanced transfer probabilities. This causes rapid depletion of the short end of the excited molecules distance distribution and time-dependent deviation of $N^*(r, t)$ from the equilibrium distribution $N_0(r)$. In essence, the combination of fast optical excitation and distance-dependent transfer rates generates a perturbation of the interprobe distances distribution from the ensemble of molecules excited at time $t = 0$. An example of the time dependence of $N^*(r, t)$ simulated for a molecule in which the interprobe distances are Gaussian distributed is shown in Fig. 1. This figure shows the fast depletion of the short distance fractions within the first few time intervals and the resulting perturbation of the shape of the distribution and the induced shift (toward longer distances) of both its maximum and average. It is important to note that no conformational perturbation is involved in this process; the conformation of the population of the labeled molecules is maintained at equilibrium. As time proceeds, the increase in the relative population of the molecules with large interprobe distances in the excited ensemble results in slower fluorescence decay rates at later times (i.e., a time-dependent rate constant). The observed result is a deviation from monoexponential decay of the donor fluorescence.

Let us now consider the effect of intramolecular Brownian motion on the time dependence of the intramolecular distance distribution function $N^*(r, t)$ (i.e., interconversions due to diffusion). Random conformational fluctuations result in an exchange of molecules between distance fractions. The higher concentrations of excited conformers with an extended interprobe distance, relative

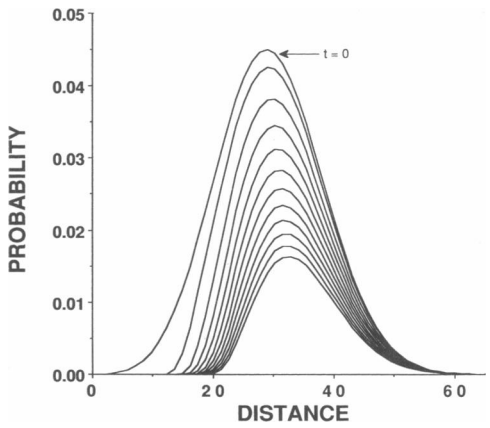

FIGURE 1 Decrease in the concentration of the excited-state donor population $N^*(r, t)$ starting at $t = 0$ with subsequent time slices every 0.4 ns. $R_0 = 27$ Å, $\tau_D = 6.0$ ns, $\tau_A = 4.0$ ns, and diffusion coefficient = 0.0. (Distance in angstroms.)

to the short distance conformers, results in a net flow of excited molecules from the longer distance fractions to the shorter ones. Those molecules are "exchanged" for nonfluorescent quenched molecules diffusing to longer distance conformations (experimentally unobserved). The perturbation of $N^*(r, t)$ is maintained by the enhanced rate of excitation transfer at the short distance conformations. The net result is that experimentally one observes a net flow of molecules from the long distance fractions to the short ones. The overall result is an enhanced decay rate of the donor. The total change with time in the concentration of excited labeled molecules of interprobe distance r, can be represented by a second order partial differential equation which takes into account both energy transfer sink term and diffusion between multiple conformations (25).

$$\frac{\partial \bar{N}(r, t)}{\partial t} = \left\{\sum_{i=1}^{n} \frac{\alpha_i}{\tau_i}\left[1 + \left(\frac{R_o}{r}\right)^6\right]\right\} \bar{N}(r, t) + \frac{1}{N_o(r)} \frac{\partial}{\partial r}\left[N_o(r) D(r) \frac{\partial \bar{N}(r, t)}{\partial r}\right], \quad (3)$$

where $N_o(r)$ is equilibrium distribution of distances between the donor and acceptor, $\bar{N}(r, t) = N^*(r, t)/N_o(r)$, and $D(r)$ is the diffusion coefficient of the two probes (relative to one another).

The first term on the right side of Eq. 3 represents both the spontaneous decay of the donor and the decrease of excited donor concentration by nonradiative energy transfer. The second term represents the replenishment of the depleted fractions by the Brownian motion of the labeled segments. The reduced distance distribution, $\bar{N}(r, t)$, obtained by solving Eq. 3 represents the time-dependent reduction of the excited donor population (normalized to $N_o[r]$) at each distance fraction taking into account both distance distributions and interconversions. A relatively simple (and fast) implicit finite difference scheme for solving Eq. 3 is presented in Appendix A.

It should be emphasized that the orientation dependence of the transfer probability (κ^2 term in Eq. 1) can further complicate the analysis of time-resolved measurements. It has been shown, however, that analysis based on an average orientation factor ($\kappa^2 = 2/3$) is correct for systems in which there is fast rotational averaging of the probes orientation. In addition, the orientational dependence of the transfer probability can be made weak or insignificant using fluorescence probes which exhibit low limiting polarization properties for the electronic transitions involved in the transfer process (28, 29). See reference 28 for a table of donor/acceptor probes which fulfill this criterion and for possible error ranges in the calculated distance distribution parameters resulting from improper κ^2 values. The following analysis is limited to the use of probes with either fast rotational averaging or mixed polarization. A more expanded version of Eq. 3, which incorporates both the Brownian diffusion term and a rotational diffusion term is currently being developed and will be presented elsewhere. See also Berger and Vanderkooi for work in this area (30).

Two examples of the solution of Eq. 3 (without and with diffusion) are shown in Figs. 2 and 3. In Fig. 2, notice the fast decrease in the population at the very short distances caused by the Förster term and the distance-independent overall decrease due to the spontaneous decay. This figure represents a typical solution of Eq. 3 when only the energy transfer sink term (first term) is considered. Fig. 3 represents the same equilibrium conformational distribution but with the additional contribution of a diffusion term ($D[r] = 20$ Å^2/ns). Note how the diffusion term replenishes the short distance highly quenched conformers. There is an accelerated reduction in the long distance fractions and an enhancement of the short distance populations. The actual observed population of molecules is represented by $\bar{N}(r, t) * N_o(r)$ and is shown in Fig. 4. One can clearly see the net effect of the Brownian motion: an increase in the short distance fractions, faster disappearance of the long distance fractions, and an apparent shift of the whole excited-state distribution (from $N_o[r]$, which is unperturbed) towards the shorter interprobe distances (as compared with the no diffusion case). By examining the solutions to this equation (with and without diffusion) one can realize why there is a strong correlation between the distance distribution and diffusion parameters. Distance distributions with diffusion cause an increase in the short distance population and hence can be compensated by a decreased distance in the static distance distribution parameters. The discrimination between a real conformational distribution with a shorter average distance and no diffusion,

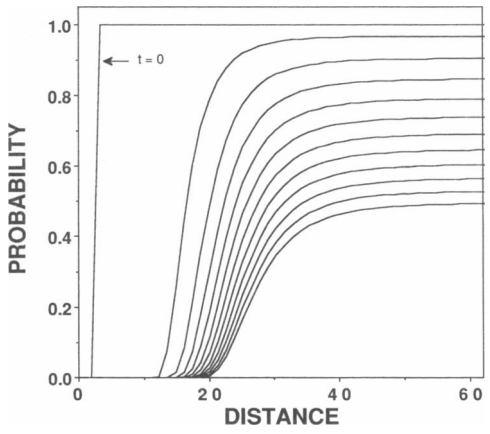

FIGURE 2 Solution of Eq. 3 for $\bar{N}(r, t)$ without diffusion. Simulation parameters same as in Fig. 1. (Distance in angstroms.)

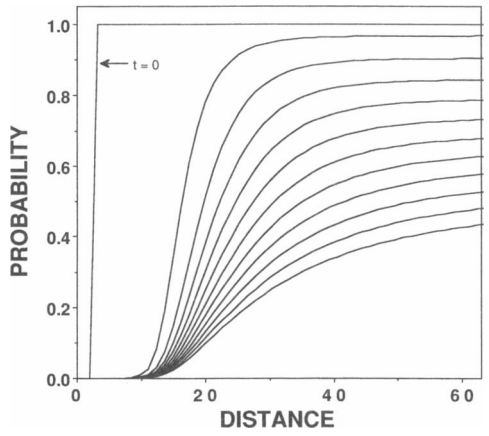

FIGURE 3 Solution of Eq. 3 for $\bar{N}(r, t)$ with diffusion. Simulation parameters same as in Figs. 1 and 2 except a diffusion coefficient of 20 Å^2/ns has been added. Note the enhanced rate of decay and the replenishment of the short distance fractions compared to the data in Fig. 2. (Distance in angstroms.)

from a longer average distance with Brownian motion of the segments, is the major objective of the present work. Although the probability distribution functions shown in Figs. 1–4 are representative of delta function excitations, the equations described below (Eqs. 4–10) are appropriate for experimentally measured excitation functions of finite width. All the simulations performed in this study utilized experimentally measured excitation functions from either flash-lamp or laser-based excitation systems.

The first step needed in performing a global analysis of the donor-acceptor decay curves is a method to calculate properly scaled donor and acceptor decay profiles. To calculate the observed time dependence of the acceptor

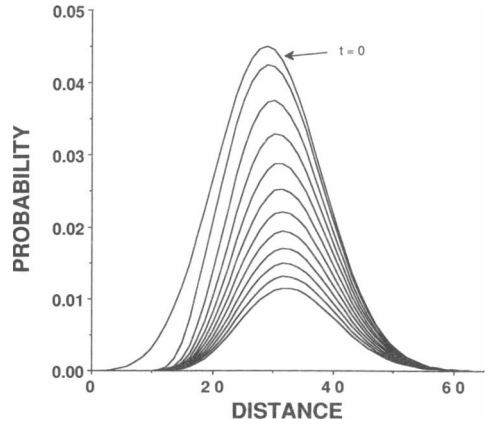

FIGURE 4 Population of excited-state molecules ($\bar{N}[r, t] * N_o[r]$) using the simulation parameters of Fig. 3 (with diffusion). (Distance in angstroms.)

population, one needs to keep track of the fraction of donor molecules escaping through the energy transfer sink term. Denoting this sink term simply as $S(r)$, one can calculate the buildup of acceptor probability as

$$P_A(r, t) = \bar{N}(r, t) * S(r) * N_o(r). \quad (4)$$

The number of acceptor molecules at any instant of time can therefore be represented as

$$N_A(t) = \int_{r_{min}}^{r_{max}} P_A(r, t)\, dr. \quad (5)$$

$N_A(0)$ equals the fraction of directly excited acceptor molecules. Note that the $N_A(t)$ which is being assembled represents the impulse response function of the acceptor in the absence of intrinsic acceptor decay but in the presence of both diffusion and energy transfer. To include the intrinsic acceptor decay terms, one must form the convolution of $N_A(t)$ with the impulse response of the acceptor in the absence of donor molecules. Denoting the acceptor impulse response function as, $i_A(t)$, one can calculate the fluorescence impulse response of the acceptor as

$$f_A(t) = N_A(t) \otimes i_A(t), \quad (6)$$

where $\otimes$ represents the convolution operator. One can then calculate the observed fluorescence signal of the acceptor as

$$F_A(t) = k_A(\lambda_{em})[f_A(t) \otimes I(t, \lambda_{ex}, \lambda_{em})] \quad (7)$$

where $I(t, \lambda_{ex}, \lambda_{em})$ represents the experimentally measured instrument response function at this particular excitation/emission wavelength region and $k_A(\lambda_{em})$ represents the emission spectral contour of the acceptor relative to the donor integrated over the spectral bandwidth of the emission monochromator/filter. The impulse response of the donor, $i_D(t)$, can be calculated as

$$i_D(t) = \int_{r_{min}}^{r_{max}} \bar{N}(r, t) * N_o(r)\, dr. \quad (8)$$

The observed donor fluorescence is then

$$F_D(t) = k_D(\lambda_{em})[I(t, \lambda_{ex}, \lambda_{em}) \otimes i_D(t)] \quad (9)$$

where $k_D(\lambda_{em})$ represents the emission spectral contour of the donor relative to the acceptor. $i_D(t)$ and $i_A(t)$, the impulse responses of the donor and the acceptor in the absence of energy transfer, are measured in independent experiments in which the same molecule is labeled either by the donor alone or the acceptor alone. The final observed fluorescence decay profile is therefore

$$F_{obs}(t, \lambda_{ex}, \lambda_{em}) = F_A(t) + F_D(t) \quad (10)$$

Having calculated the predicted fluorescence decay of

the donor alone, acceptor alone, and the donor-acceptor pairs as a function of emission wavelength, a global analysis can be performed. The mechanics of implementing a global analysis of multidimensional fluorescence data surfaces has been previously described in detail (15, 18, 19, 22–24). For energy transfer experiments, there is a very simple linkage scheme between the various experiments, in that one examines data at multiple excitation/emission wavelengths in terms of an internally consistent distance distribution and diffusion parameter(s) with varying spectral parameters.

RESULTS

Three conformational distribution parameters which strongly affect the rates of nonradiative energy transfer between donor and acceptor pairs can be obtained by the global analysis of the fluorescence decay curves of the energy transfer probes: the average interprobe distance, the width and shape of the interprobe distance distribution function(s), and the rates of changes of the interprobe distances either by Brownian motions (fluctuations within the equilibrium distributions) or by vectorial conformational changes.

Vectorial conformational transitions can be detected either when experimentally initiated, and hence synchronized, by the excitation pulse, or, when caused by a fast perturbation (i.e., heat, denaturant, pH, etc.) which causes a reaction to persist during the time interval of data collection (e.g., unfolding or refolding of a protein). In the present communication we shall restrict our discussion and simulations to Brownian conformational dynamics, yet it should be emphasized that the current global analysis framework will allow the examination of physical perturbation studies also.

Three distinct time windows are defined by any particular donor acceptor pair in an energy transfer experiment: (*a*) Static regime: contribution of the dynamic conformational changes to the rate of energy transfer are small (very low diffusion occurring during the lifetime of the excited state). (*b*) Intermediate regime: many (but not all) distance fractions interconvert during the excited state lifetime. (*c*) Fast dynamics regime: fast fluctuations enable most conformers to sample all allowed distances (including the shortest ones) within the lifetime of the excited state.

An energy transfer experiment should be designed for the intermediate time regime window if both distance distributions and diffusion constants are of interest. Experiments performed in the static regime, allow only an upper limit for the value of the intramolecular diffusion constant to be determined. It is only in this region that one can utilize Eq. 2 to recover the correct equilibrium interprobe distances distribution function. In the fast dynamics regime, all states can be sampled many times within the lifetime of the donor excited state. Analysis of these types of experiments using Eq. 2 yields distance parameters which are strongly shifted (to shorter distances) from the actual equilibrium distances experienced by the sample being examined. Using global analysis (with Eq. 3) only a lower limit for the intramolecular diffusion constant can be determined, yet the correct parameters of the equilibrium distance distributions are recovered. In the intermediate regime, when the diffusion rate is moderate, both the distance distribution parameters and the diffusion term(s) can be accurately recovered. It should be reemphasized that the classification of an experiment into one of the above regimes is mainly a function of the given diffusion rates and the lifetime of the donor excited state. One can thus select a fluorescent probe with suitable excited state lifetime and R_0 to design the experiment for optimal sensitivity.

The strength of the new global analysis method is in determination of both intramolecular diffusion constants and distance distributions and was tested by the following simulation. An experiment in the intermediate time regime was simulated with a Gaussian equilibrium distance distribution and a distance-independent diffusion coefficient of 20 $Å^2$/ns. Decay curves of 20,000 counts at the peak (500 channels) were simulated at a timing calibration of 0.05 ns/channel and photon counting noise was added (i.e., a typical low-resolution fluorescent decay experiment). The simulated data were analyzed using a single experiment donor-only decay analysis, and by performing a simultaneous analysis of the four experiments: donor-only, acceptor-only, donor emission of donor/acceptor pair, acceptor emission of donor/acceptor pair. Individual analysis of the donor-only decay curve required that *a priori* values of the donor and acceptor lifetimes be fixed in the analysis as known quantities. This was done, and both donor and acceptor lifetimes were fixed at exactly their proper values. In the global analysis, the lifetimes of the donor and acceptor were not fixed *a priori,* but were actual fitting parameters in the analysis along with both the distance distributions and the diffusion coefficient.

Upon performing the single experiment donor-only analysis, it was found that a wide variety of diffusion coefficients and distance distributions could be recovered (depending on the initial guess) with essentially identical error statistic (χ^2) values. The global analysis procedure, however, always converged to the proper diffusion coefficient *and* distance distribution. We were interested in rigorously estimating the errors associated with the recovery of the fitting parameters using the global and donor-only analyses methods. It has become standard practice in the fluorescence decay community (and in many other

areas) to estimate the errors in the recovered parameters using the square root of the diagonal elements of the inverse of the covariance matrix (SD error$_i$ = $\pm\sqrt{C_{ii}^{-1}}$) (28). This type of error analysis only applies for linear models, and therefore will grossly underestimate the uncertainties in the recovered parameters (31, 32). To test the global and donor only analysis methods, it was decided to perform a completely rigorous error analysis by directly examining the error surfaces associated with the two methods.

To perform an absolutely rigorous error estimate on the ith fitting parameter, one can systematically fix this parameter at a series of values, and perform an entire nonlinear minimization, allowing the remaining $n - 1$ parameters to vary to minimize χ^2. One can then record the series of minimum χ^2 values possible over a particular range of the ith fitting parameter. Although this method requires a whole series of nonlinear analyses to be performed, it is absolutely rigorous, because it takes into account all of the higher order correlations which may exist between a given set of fitting parameters (i.e., all other parameters are allowed to compensate for each particular change imposed on the parameter of interest). The results of these error analyses performed on the global and donor only analyses of the diffusion coefficients and the mean/width of the distance distributions are presented in Figs. 5–7.

In each of these figures, it is clearly evident that the donor-only analysis has an error surface which is very ill determined. This is the reason why the individual curve analysis was very dependent upon the initial guess. One can terminate analysis at a whole series of different

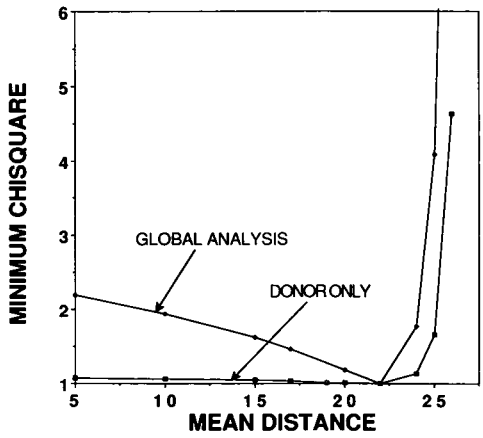

FIGURE 6 Minimum possible chisquare error value as a function of the mean of the distance distribution as described in the text. The synthesized value for the mean distance is 22 Å. The donor analysis method can only set an upper limit to the mean distance whereas the global analysis error surface is very well defined.

means, widths, and diffusion coefficients with essentially no change in χ^2. The global analysis error surfaces, however, are much better defined, show distinct minima, and recover the input simulation values with the following uncertainties: $20 < r_{mean} < 22.5$ Å (synthesized = 22), width of distribution = $9 < \sigma_r < 12.5$ Å (synthesized = 10), and diffusion coefficient = $18 < D < 25$ Å^2/ns (synthesized = 20). The error surfaces are all very asymmetric, but they do not contain multiple minima. The errors on the recovered global analysis parameters are estimated using the F-statistic (at the 99% confidence

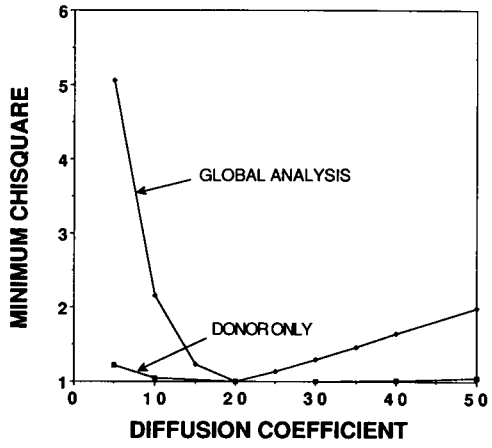

FIGURE 5 Minimum possible chisquare error value as a function of diffusion coefficient obtained as described in the text. The synthesized value for the diffusion coefficient is 20 Å^2/ns. The donor analysis method can only set a lower limit to the diffusion whereas the global analysis error surface is very well defined.

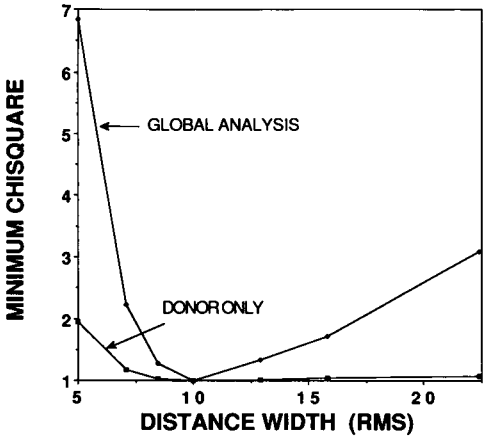

FIGURE 7. Minimum possible chisquare error value as a function of the width of the distance distribution as described in the text. The synthesized value for the width (root mean squared) is 10 Å. The donor analysis method can only set a lower limit to the width whereas the global analysis error surface is very well defined.

level). The F-statistic is simply a convenient guide in choosing a particular region of constant χ^2 contour. Although the confidence levels are approximate, the actual error surfaces plotted in Figs. 5–7 are exact. Determining the upper and lower error bars on the parameters simply amounts to drawing a horizontal line across the graphs and projecting the intersections of the χ^2 curves with the abscissa. The approximation involved in using the F-statistic is simply deciding how far up the ordinate this line should be placed. What should be clear from these figures is that independent of where the confidence level is set, the global analysis method has a well-defined error surface whereas the donor-only analysis does not. In each case, the donor-only analysis of the data could not significantly recover the diffusion coefficient, or the mean/width of the distribution in a statistically significant manner. The global analysis of the data set, is able to recover, in a statistically significant manner, both the distance distribution parameters and the diffusion coefficient.

As an extra test concerning the the proper operation of the computer algorithm for the calculation of the observed fluorescence responses, donor and acceptor fluorescence decay curves were simulated for the following special energy transfer cases (where some analytical results exist): $r_{mean} \ll R_o$, $r_{mean} \gg R_o$, and a narrow distance distribution with $r = R_o$. In all simulations D was set to 20 Å^2/ns, $\tau_D = 6$ ns and $\tau_A = 4$ ns. The ratio of donor total fluorescence to the total fluorescence (i.e., integrated area under the decay curves) was found to be 0.0001, or 0.99997, and 0.5, respectively. This is the expected result which predicts: total transfer, no transfer, and 50% transfer. In addition, the decay kinetics from the $r = R_o$ narrow distribution case, analyzed very well as a single exponential donor decay and double exponential acceptor decay (with equal and opposite amplitudes). Hence these simulations confirm that all terms in the model are well scaled (i.e., all photons in the system can be accounted for) and that the analytical solution from elementary kinetics can be obtained as limiting case solution to Eq. 3. The diffusion equation solver written for Eq. 3 (described in the Appendix) was tested against the general purpose partial differential equation solver DPDES (IMSL, Inc., Houston, TX). It was found that the numerical solutions determined by either method were identical.

DISCUSSION

In the present study we are interested in determination of intramolecular distances distribution functions and rates of intramolecular Brownian motions. The experimental approach is based on measurements of the time-dependent rates of nonradiative energy transfer between probes located at sites whose relative positions and motions are of structural interest. The physical basis for the experimental method is the distance dependence of the nonradiative energy transfer rates. Provided that all other spectral parameters are conformationally invariant (which is tested by other methods in control experiment [33]), changes in transfer rates can be analyzed in terms of intramolecular distances and diffusion.

Comparison of Figs. 1 and 2 with Figs. 3 and 4 clearly demonstrate that shape of the function $N^*(r, t)$ is altered by the segmental diffusion of the labeled sites. The simulations and analyses reported above show that the global analysis of energy transfer experiments can utilize the resulting differences in the shape of $N^*(r, t)$ to significantly distinguish the static and dynamic contributions to the rates of energy transfer. Donor-only analysis methods were insensitive to these subtle shape changes. The simultaneous global analysis, however, is sensitive enough to take advantage of the fine structure differences in the shape of the measured fluorescence decay curves and yield fitting parameters with high statistical significance. The error analysis method utilized to examine the confidence intervals in the recovered parameters revealed that the global solutions are well defined and do not have multiple minima (error surfaces were examined much farther from the minima than shown in graphs).

It is important to bear in mind that knowledge of the role of the key parameters in the analysis can help in establishing a useful experimental design (e.g., determination of static, intermediate, and fast diffusion regimes). The experimental design parameters consist of the molecular distances and diffusion coefficients of interest, the photophysical properties of the donor/acceptor probes, and the instrumental detection system. Each of these components has a characteristic time and distance "window," or range, of optimal sensitivities. The optimal distance sensitivity is a function of the ratio of the average and width of the distance distribution(s) and R_o. Eqs. 1 through 3 show that maximal change in the rate of transfer is obtained when $r_{mean} \approx R_o$. R_o is in principle (and practice) the length scale of the experiment. The optimal time sensitivity for determination of parameters of conformational dynamics by the present method is a function of the donor lifetime. When the contribution of the energy transfer and the diffusion terms of Eq. 3 are comparable with the donor decay rate, the analysis is most sensitive to the magnitude of the diffusion coefficient. As mentioned above, the Förster energy transfer term generates the virtual concentration gradient in the population of molecules carrying an excited donor probe at any time interval, while the Fick term is responsible for restoration of the equilibrium distribution (fluctuations within the equilibrium conformational distribution are equivalent to diffusion under a force field). If the balance

between these two terms is such that the first one is dominant, it is difficult to distinguish the dynamic experiment from a static (frozen) one and the information about the diffusion is lost in the noise. On the other hand, if the Fick term is dominant, fast replenishment of the depleted short-distance fractions takes place. The distribution of donor excited molecules found at each time interval will therefore have approximately the same shape as the equilibrium distribution, $N_o(r)$, except for reduced area. This is the case of the fast diffusion regime, and in such a situation the analysis is unable to distinguish the dynamic model from a simple static model with a shorter average distance. The diffusion parameter obtained in that case shows a very broad error minimum and cannot be determined with reasonable statistical significance. Hence maximal sensitivity is obtained when the experiment is conducted in the intermediate time regime. Therefore, one should attempt to select for a pair of donor/acceptor probes with characteristic R_o and donor excited state lifetime, which match the range of distances and diffusion rates expected for the investigated molecules.

The additional benefits of monitoring acceptor emission and its decay rate are twofold. First a technical detail: the spectral separation between the donor excitation and acceptor emission bands is by definition larger than that of donor excitation and emission bands. This results in an improved signal to noise when examining the acceptor fluorescence because all scattering, Raman and fluorescence background emissions are thus much reduced. Secondly, in the donor emission, the fractions of molecules with the shortest interprobe distances can decay very fast. In most conventional time-resolved fluorometers it is difficult to get an exact quantitation of the amplitudes of contributions of the very fast decay components which disappear within very few channels. Those fractions are thus recovered with poor accuracy from analysis of the donor fluorescence decay curve, even in the static regime. The acceptor emission, however, captures those processes with high sensitivity, due to the additional convolution with the acceptor impulse response (Eq. 4), which effectively "spreads" this information out over a much larger time interval. A similar argument holds for the weighting of the emission from the fractions with large (relative to R_o) interprobe distances. These long distances contribute a weak signal to the acceptor emission but are well weighted in the donor emission. Thus, combination of both donor and acceptor emission data complement one another very well and can drastically improve the determination of the fitting parameters. It should be pointed out that even more accuracy and statistical confidence in the determined parameters can be obtained by combining a series of experiments in which temperature/viscosity is changed in a controlled manner by mild changes in the physical environment. A change in temperature (or viscosity) over a limited range enhances the dynamic diffusive contributions without changing the equilibrium conformation (dependent upon the particular system). Global analysis of these multiple experiments can further reduce the uncertainty in the recovered parameters.

Another physical parameter than can be changed to aid in experimental design is the intrinsic lifetime of the donor and acceptor (τ_D, τ_A). The lifetimes can be reduced, with a concomitant reduction in R_o, by addition of quenchers to the solution. Both τ_D and R_o are changed in a manner controlled by the quencher concentration and are determined by combining the associated experiments in which both τ_D and τ_A are measured in the absence of energy transfer. A series of experiments can be globally analyzed in which all four associated experiments, donor and acceptor decay curves with and without energy transfer (double- and single-labeled derivatives), are collected for each quencher concentration. Analysis is performed in terms of an internally consistent set of Brownian motions and distance distributions and decay rate "sink-terms" which follow an appropriate quenching law (e.g., Stern-Volmer kinetics). Analysis of this type of data from steady-state energy transfer experiments has recently been described (34).

In the diffusion model, simulations have been performed where the diffusion coefficient is not constant as a function of the donor-acceptor distance. In one model, a linear increase of the diffusion rate with distance was introduced ($D(r) = D_o + a * r$), thereby modeling the less folded conformers as having less internal frictional forces (25). In another model, a harmonic potential type dependence was simulated (inverted parabola), in which the diffusion rate is highest at the average of the intramolecular distances distribution. This type of "diffusion" may be useful in the analysis of intramolecular fluctuations in proteins which exhibit very fast transitions between states. The additional flexibility of, $D = D(r)$, provided by the solutions given in the Appendix allows for a very simple introduction of these types of models. The identifiability of these more complicated diffusion models is currently under investigation. The error surfaces described in this paper have all been generated using a distance-independent diffusion coefficient.

Simulation studies performed with multiple donor and acceptor lifetimes reveal that the individual curve error surfaces become even more ill-defined. The global error surfaces (although not as steep) are still well defined and do not show multiple minima. However, when examining cases of multi- (or even distributed) exponential decay from the donor or acceptor it should be kept in mind that Eq. 3 (as written) represents a "nonassociative" sink term (i.e., each lifetime and amplitude is independent of r). For the associative case one simply replaces the α_i term with

$\alpha_i(r)$. Similarily, for the acceptor term, the integral in Eq. 5 must be broken into multiple pieces to form $N_{A_j}(t)$, where the jth index keeps track of the impulse response appropriate over each particular distance region. Eq. 6 then becomes a sum over the j distance-dependent impulse response functions of the acceptor.

In this study, only parameterized unimodal Gaussian distribution functions describing the distance distribution(s) have been utilized. Other conformational distribution shapes will have different errors associated with their recovery. Lorentzian distributions can be determined with less error than Gaussians, whereas, gamma distributions tend to have slightly larger confidence intervals. The actual choice of the parameterization function describing the distribution is not extremely critical in the analysis. Data simulated with a particular parameterized distribution function and analyzed in terms of a different parameterization will generally still yield acceptable fitting results. The analysis program will alter the fitting elements of a particular parameterization so as to obtain the largest amount of overlap of the two different distance distribution functions. Therefore, analysis with different distribution parameterizations usually results in the recovery of very similar model parameters. However, for analysis with complicated diffusion behavior ($D = D[r]$), the choice of a proper distribution type (based on theoretical analysis of the particular system being examined) will be more critical. For instance, a distribution which is "skewed" to shorter distances can be fit to a nonskewed distance distribution but with an increased diffusion function at short distances. The use of nonparameterized distance distributions (e.g., using maximum entropy techniques [35]) may be beneficial in the analysis of energy transfer experiments when no theoretical distance distribution functions are available.

It should be emphasized that all types of global analyses, which involve the linking together of multiple experiments in terms of an internally consistent framework, require a model-dependent aspect. The model-dependent aspects of the analysis provided in this paper utilize Förster type transfer, Fick's diffusion equation, and parameterized distance distributions and diffusion coefficients. Of these three, perhaps only Förster type transfer has been rigorously established as appropriate for biological macromolecules. However, this simplistic model framework provides an analytical tool to assist the experimentalist in interpreting the observed complex decay kinetics in terms of physical parameters (not just amplitudes and relaxation times). The complete characterization of the intramolecular dynamics and conformational heterogeneity in a particular protein system will undoubtedly require an extended global analysis utilizing multiple temperature/viscosity states, multiple donor/acceptor dyes, multiple quenchers, etc. Given the mathematical and physical framework presented in this paper, these additional experimental axes can be immediately incorporated into existing global analysis minimization algorithms (15). It is only with these additional experimental/analysis approaches, that better defined limits of conformation distribution shapes and interconversion rates will be determined.

In conclusion, the present method of data analysis for energy transfer experiments, provides a new tool for the determination of equilibrium distance distributions and associated fluctuations. A wide range of conformational transitions rates and intramolecular distances distributions can be found in biological macromolecules, although very few systems have been experimentally characterized. It was our interest in the protein folding and dynamics problem that motivated the developments that are reported here. We are confident that many others fields in polymer and biopolymer research can apply this approach as well.

APPENDIX

The implicit finite difference form of Eq. 3 can be represented as (36–38)

$$\frac{(\bar{N}_r^{t+1} - \bar{N}_r^t)}{\Delta t} = \frac{1}{N_o(r)} \cdot \left[\frac{a_{r+1/2}\bar{N}_{r+1}^{t+1} - (a_{r+1/2} + a_{r-1/2})\bar{N}_r^{t+1} + a_{r-1/2}\bar{N}_{r-1}^{t+1}}{(\Delta r)^2}\right] + \left[\sum_i^n \frac{\alpha_i}{\tau_i}\left(1 + \left(\frac{r_o}{r}\right)^6\right)\right]\bar{N}_r^t, \quad (11)$$

where $a_r \equiv D_r * N_{or}$.

These equations can be solved "forward" in time by isolating the $\bar{N}^{t+1}$ terms, which results in a tridiagonal system of equations to solve.

The boundary conditions appropriate for this problem are as follows.

$$\bar{N}(0, r) = 1.0 \quad (12)$$

$$\bar{N}(t, r_{min}) = 0.0 \quad \text{or} \quad \frac{\partial \bar{N}}{\partial r}\Big|_{r=r_{min}} = \beta \quad (13)$$

$$\frac{\partial \bar{N}}{\partial r}\Big|_{r=r_{max}} = 0.0. \quad (14)$$

The outer boundary condition is represented as a reflecting barrier. The inner boundary condition is either of the Schmoulokowski type ($\bar{N}[t, r_{min}] = 0.0$) or a reflecting ($\beta = 0$) or partially reflecting ($\beta \neq 0$) barrier (depending on the physical system examined). A reflecting inner boundary condition was utilized in these simulations.

J. M. Beechem gratefully acknowledges support from the Lucille P. Markey Foundation. J. M. Beechem is a Lucille P. Markey Scholar in Biomedical Sciences. The Laboratory for Fluorescence Dynamics (LFD) is supported jointly by the Division of Research Resources of the National Institutes of Health (RR03155-01) and the University of Illinois Urbana-Champaign. E. Haas gratefully acknowledges the sup-

port of the National Institutes of Health General Medical Sciences (NIH grants R01-GM39372-01 and R01-GM41360-01) and the United States-Israel Bi-national Science Grant Foundation (grant 217/84).

Received for publication 25 July 1988 and in final form 2 February 1989.

REFERENCES

1. Cooper, A. 1984. Protein fluctuations and the thermodynamics uncertainty principle. *Prog. Biophys. Mol. Biol.* 44:181–214.
2. Karplus, M., and J. A. McCammon. 1981. The internal dynamics of globular proteins. *CRC Crit. Rev. Biochem.* 9:292–349.
3. Elber, R., and M. Karplus. 1987. Multiple conformational states of proteins: a molecular dynamics analysis of myoglobin. *Science (Wash. DC).* 235:318–321.
4. Austin, R. H., K. W. Beeson, L. Eisenstein, H. Frauenfelder, and I. C. Gunsalus. 1985. Dynamics of ligand binding to myoglobin. *Biochemistry.* 14:5355–5373.
5. Elson, E. L., and D. Magde. 1974. Fluorescence correlation spectroscopy. 1. Conceptual basis and theory. *Biopolymers.* 13:1–27.
6. Förster, T. 1948. Zwischenmolekulare Energiewanderung und Fluoreszenz. *Ann. Phys. (Leipzig).* 2:55–75.
7. Stryer, L., and R. P. Haugland. 1967. Energy transfer: a spectroscopic ruler. *Proc. Natl. Acad. Sci. USA.* 58:719–726.
8. Haas, E., M. Wilchek, E. Katchalski-Katzir, and I. Z. Steinberg. 1975. Distribution of end-to-end distances of oligopeptides in solution as estimated by energy transfer. *Proc. Natl. Acad. Sci. USA.* 72:1807–1811.
9. Steinberg, I. Z., E. Haas, and E. Katchalski-Katzir. 1984. Long range nonradiative transfer of electronic excitation energy. *In* Time Resolved Fluorescence Spectroscopy in Biochemistry and Biology. Vol. 69. R. B. Cundall and R. E. Dale, editors. Plenum Publishing Corp., New York. 411–451.
10. Haas, E., and I. Z. Steinberg. 1984. Intramolecular dynamics of chain molecules monitored by fluctuations in efficiency of excitation energy transfer. *Biophys. J.* 46:429–437.
11. Grinvald, A., E. Haas, and I. Z. Steinberg. 1972. Evaluation of the distribution of distances between energy donors and acceptors by fluorescence decay. *Proc. Natl. Acad. Sci. USA.* 69:2273–2277.
12. Lakowicz, J. R., M. L. Johnson, W. Wiczk, A. Bhat, and R. F. Steiner. 1987. Resolution of a distribution of distances by fluorescence energy transfer and frequency-domain fluorometry. *Chem. Phys. Lett.* 138:587–593.
13. Cheung, H. C., C. Wang, I. Gryczynski, M. L. Johnson, and J. R. Lakowicz. 1988. Distribution of distances in native and denatured troponin I, from frequency-domain measurements of fluorescence energy transfer. *Proc. Int. Soc. Opt. Engin. (SPIE).* 909:163–169.
14. Lanczos, C. 1956. Applied Analysis. Prenctice-Hall, Englewood Cliffs, NJ. 272.
15. Beechem, J. M., and E. Gratton. 1988. Fluorescence spectroscopy data analysis environment: a second generation global analysis program. *Proc. Int. Soc. Opt. Engin. (SPIE).* 909:70–81.
16. Johnson, M. L., H. R. Halvorson, and G. K. Ackers. 1976. Oxygenation-linked subunit interactions in human hemoglobin: analysis of linkage functions for constituent energy terms. *Biochemistry.* 15:5363–5371.
17. Parodi, L. A., R. H. Lozier, S. M. Bhattacharjee, and J. F. Nagel. 1984. Testing kinetic models for the bacteriorhodopsin photocycle. II. Inclusion of an O to M back reaction. *Photochem. Photobiol.* 40:501–512.
18. Knutson, J. R., J. M. Beechem, and L. Brand. 1983. Simultaneous analysis of multiple fluorescence decay curves: a global approach. *Chem. Phys. Lett.* 102:501–507.
19. Beechem, J. M., J. R. Knutson, J. B. A. Ross, B. W. Turner, and L. Brand. 1983. Global resolution of heterogeneous decay by phase/modulation fluorometry. *Biochemistry.* 25:599–607.
20. Beechem, J. M., M. Ameloot, and L. Brand. 1986. Global analysis of fluorescence decay surfaces: excited-state reactions. *Chem. Phys. Lett.* 120:466–472.
21. Ameloot, M. A., J. M. Beechem, and L. Brand. 1986. Simultaneous analysis of multiple fluorescence decay curves by Laplace transforms: deconvolution with respect to reference and excitation profiles. *Biophys. Chem.* 23:155–171.
22. Beechem, J. M., M. A. Ameloot, and L. Brand. 1988. Analysis of fluorescence intensity and anisotropy decay surfaces. *In* Excited-State Probes in Biochemistry and Biology. A Szabo and L. Masotti, editors. Plenum Publishing Co., New York.
23. Beechem, J. M., E. Gratton, M. A. Ameloot, J. R. Knutson, and L. Brand. 1989. The global analysis of fluorescence intensity and anisotropy decay data: second generation theory and program. *In* Fluorescence Spectroscopy: Analysis and Instrumentation. Vol. 1. J. R. Lakowicz, editor. Plenum Publishing Corp., New York.
24. Beechem, J. M., M. Ameloot, and L. Brand. 1985. Global analysis of complex decay phenomena. *Anal. Instrum.* 14:379–402.
25. Haas, E., E. Katchalski-Katzir, and I. Z. Steinberg. 1978. Brownian motion of the ends of oligopeptides chains in solution estimated by energy transfer between the chain ends. *Biopolymers.* 17:11–31.
26. Gekko, K., and S. N. Timasheff. 1981. Thermodynamic and kinetic examination of protein stabilization by glycerol. *Biochemistry.* 20:4677–4686.
27. Amir, D., and E. Haas. 1987. Estimation of intramolecular distances distributions in bovine pancreatic trypsin by site-specific labeling and non-radiative excitation energy transfer measurements. *Biochemistry.* 26:2162–2175.
28. Haas, E., E. Katchalski-Katzir, and I. Z. Steinberg. 1978. Effect of the orientation of donor and acceptor on the probability of energy transfer involving transitions of mixed polarization. *Biochemistry.* 17:5064–5070.
29. Stryer, L. 1978. Fluorescence energy transfer as a spectroscopic ruler. *Annu. Rev. Biochem.* 47:819–846.
30. Berger, J. W., and J. M. Vanderkooi. 1988. Brownian dynamics simulation of intramolecular energy transfer. *Biophys. Chem.* 30:257–269.
31. Bevington, P. R. 1969. Data Reduction and Error Analysis for the Physical Sciences. McGraw-Hill Book Co., New York.
32. Johnson, M. L. 1983. Evaluation and propagation of confidence intervals in nonlinear, asymmetric variance spaces. *Biophys. J.* 44:101–106.
33. Haas, E. 1986. Folding and dynamics of proteins studied by non-radiative energy transfer measurements. *In* Photophysical and Photochemical Tools in Polymer Science. M. A. Winnik, editors. D. Reidel, Dordrecht, FRG. 316–341.
34. Gryczynski, I., W. Wiczk, M. L. Johnson, H. C. Cheung, C. Wang, and J. R. Lakowicz. 1988. Resolution of end-to-end distance

distributions of flexible molecules using quenching-induced variations of the Forster distance for fluorescence energy transfer. *Biophys. J.* 54:577–586.

35. Livesey, A. K., and J. C. Brochon. 1987. Analyzing the distribution of decay constants in pulse-fluorimetry using the maximum entropy method. *Biophys. J.* 52:693–706.
36. Press, W. H., B. P. Flannery, S. A. Teukolsky, and W. T. Vetterling. 1986. Numerical Recipes (Fortran Version). Cambridge University Press, Cambridge, UK. 635–640.
37. Koonin, S. E. 1986. Computational Physics. Addison-Wesley Publishing Co., Reading, MA. 165–169.
38. Ames, W. F. 1969. Numerical Methods for Partial Differential Equations. Academic Press, Inc., New York. 49–54.